Med. J. Kagoshima Univ., Vol. 65, No. 1, 9–18 May, 2013

^{99m}Tc Pertechnetate Scintigraphy for Warthin Tumors of the Parotid Gland: Comparison of Histopathological and Magnetic Resonance Imaging findings

Megumi Jinguji, MD, PhD*, Hiroaki Tanabe, MD*, Masayuki Nakajo, MD, PhD*, Yoshiaki Nakabeppu, MD, PhD*, Yoshihiko Fukukura, MD, PhD*, Shoji Matsune, MD, PhD†, Takako Yoshioka MD, PhD‡

Departments of *Radiology, †Otolaryngology, and ‡Molecular and Cellular Pathology,
Kagoshima University Graduate School of Medical and Dental Sciences, Kagoshima, Japan

(Accepted 8 February 2013)

Abstract

Purpose: To examine the relationships between degrees of ^{99m}Tc pertechnetate ($^{99m}TcO_4^-$) uptake after acid stimulation and the tumor size as well as histopathological subtypes of Warthin tumor and to evaluate the diagnostic accuracy of $^{99m}TcO_4^-$ scintigraphy and routine magnetic resonance (MR) imaging in differentiating Warthin and non-Warthin tumors of the parotid gland.

Methods: We reviewed a total of 83 pathologically proven parotid gland tumors in 79 patients (37 Warthin tumors and 46 non-Warthin tumors) that had been resected after $^{99m}TcO_4^-$ scintigraphy with acid stimulation. Of these, MR imaging was performed in 53 patients before surgery (21 Warthin tumors and 33 non-Warthin tumors), among which contrast-enhanced dynamic MR imaging was also performed in 50 patients (20 Warthin tumors and 30 non-Warthin tumors). The Kruskal–Wallis test was used to compare visually scored degrees of $^{99m}TcO_4^-$ uptake with tumor size and histopathological subtypes (epithelial components of 70%–80%, 40%–60%, and 20%–30%) in 37 Warthin tumors. The findings of T2-weighted and contrast-enhanced dynamic MR imaging were evaluated for the differential diagnosis of Warthin and non-Warthin tumors. We used the proportional test to compare the accuracy of $^{99m}TcO_4^-$ scintigraphy, T2-weighted MR imaging, and contrast-enhanced dynamic MR imaging in diagnosing Warthin tumor.

Results: $^{99m}TcO_4^-$ uptake in Warthin tumors showed marginal but statistically insignificant associations with tumor size (P = 0.092) and tumor pathological subtype (P = 0.070). Of the 8 false-negative tumors, 6 contained 1 or more of the following changes: hemorrhage, hyaline or cystic degeneration, fibrosis, and infarction. A metastatic atypical meningioma showed false-positive uptake. The diagnostic accuracy was 89% for scintigraphy (sensitivity, 78%; specificity, 98%), 81% for T2-weighted MR imaging (sensitivity, 81%; specificity, 82%), and 82% for contrast-enhanced dynamic MR imaging (sensitivity, 60%; specificity, 97%); significant differences in the diagnostic accuracy among the modalities were absent (P = 0.37).

Conclusions: $^{99m}TcO_4^-$ uptake in Warthin tumors does not appear to depend solely on the tumor size or histological subtype and may be affected by nonviable parenchymal changes in the tumors. Scintigraphy may be equal to T2-weighted and contrast-enhanced dynamic MR imaging in differentiating Warthin and non-Warthin tumors.

Key words: parotid tumor, Warthin tumor, $^{99m}TcO_4^-$ scintigraphy, magnetic resonance imaging.

Corresponding author: Dr. Megumi Jinguji, MD, PhD
Address: Department of Radiology, Kagoshima University Graduate School of Medical and Dental Sciences, 8-35-1 Sakuragaoka, Kagoshima 890-8544, Japan
E-mail: megu@m.kufm.kagoshima-u.ac.jp

Introduction

Warthin tumor, the second most common benign parotid tumor, accounts for 4%–25% of all salivary gland tumors[1]. Preoperative diagnosis of Warthin tumor is important for surgical management[2]. ^{99m}Tc pertechnetate ($^{99m}TcO_4^-$) salivary gland scintigraphy is a simple, noninvasive and useful method for detection and diagnosis of Warthin tumors[2]. Warthin tumors are typically imaged as hot nodules on $^{99m}TcO_4^-$ scintigraphy[1, 3]. However, $^{99m}TcO_4^-$ does not always accumulate in Warthin tumors[4-6]. The uptake of $^{99m}TcO_4^-$ is thought to be increased because of the ability of epithelial cells in Warthin tumor to extract large anions such as pertechnetate from the blood[2, 7]. The proportion of epithelial and lymphoid components varies among Warthin tumors. Seifert et al. subclassified Warthin tumors into 4 types according to the ratio of epithelial component to lymphoid stroma[8]: typical, stroma-poor, stroma-rich and the others (metaplastic). However, only a few studies have examined the degree of $^{99m}TcO_4^-$ uptake relating to the tumor size and epithelial content[6, 9].

Magnetic resonance (MR) imaging has also been reported to be useful in the evaluation of Warthin tumors, which typically show hypointensity in T2-weighted MR imaging[10, 11] as well as early enhancement and high washout rate on dynamic contrast-enhanced MR imaging[10-12]. However, there are few studies comparing the diagnostic accuracy of $^{99m}TcO_4^-$ scintigraphy and MR imaging for Warthin tumors[10].

The present study aimed to examine the relationships between degrees of $^{99m}TcO_4^-$ uptake with the tumor size and histological subtype of Warthin tumors and compare the accuracy of $^{99m}TcO_4^-$ scintigraphy and MR imaging for the diagnosis of Warthin tumors.

Materials and Methods

Patients

Our retrospective study had institutional review board approval, and the need for informed consent was waived. We reviewed 83 parotid tumors with pathologically confirmed diagnoses that had been surgically excised after $^{99m}TcO_4^-$ scintigraphy in 79 patients between January 2000 and December 2006. The patient population was composed of 44 men and 35 women, with a mean age of 59.3 years (range, 13–83 years). Of the 79 patients, 75 had a one-sided parotid tumor and 4 had bilateral tumors. Two patients had multiple Warthin tumors on the same side, which were regarded as one parotid tumor. The 83 tumors consisted of 37 Warthin tumors, 28 pleomorphic adenomas, 5 lymphoepithelial cysts, 5 basal cell adenomas, and one each of the followings: oncocytoma, neurofibroma, salivary duct cyst, epithelial–myoepithelial carcinoma, metastasis of atypical meningioma, cystic lymphoid hyperplasia, adenocarcinoma, and cavernous hemangioma.

$^{99m}TcO_4^-$ scintigraphy

After intravenous injection of the tracer [370 MBq (10 mCi) of $^{99m}TcO_4^-$] with the patient in the supine position, 60 s/frame anterior and posterior image data were acquired for 40 min using either a dual-headed gamma camera (Prism 2000, Shimadzu, Kyoto, Japan) with low-energy, multiparallel hole collimators or a dual-headed gamma camera (E.CAM, Toshiba, Tokyo, Japan) with low-medium energy, general purpose collimators. A small amount (2 cc) of citric acid or acetic acid was dropped into the patient's mouth as a taste stimulation agent 30 min after intravenous injection of the tracer. Anterior, posterior, and bilateral static images were obtained for 5 min after dynamic image data acquisition.

MR imaging techniques

MR imaging examinations were performed by using a 1.5-T MR unit (Magnetom Vision, Siemens, Germany) with a neurovascular array coil. T2-weighted turbo-spin echo images [repetition time (TR), 3474–4500 ms; effective echo time (eTE), 99 ms; echo train length (ETL), 11] of the transverse plane were obtained with a section thickness of 5–6 mm. Dynamic contrast-enhanced images were obtained in the transverse or coronal planes. First, gadolinium chelate (0.5 mmol/mL) was intravenously administered at a rate of 2.0 mL/s followed by 20 mL saline flush, and then T1-weighted turbo spin echo images (TR, 300–348 ms; eTE, 12 ms; ETL, 3; slice thickness, 3–6 mm) of 8 serial sets of images during 120–180 s, T1-weighted turbo spin echo images (TR, 302–483 ms; eTE, 12 ms; ETL, 3; slice thickness, 4 mm) of 4 serial sets of images at 25, 65, 120, and 180 s, or turbo fast low-angle shot images (flip angle, 75°; TR, 117.3 ms; eTE, 4.1 ms; slice thickness, 3–6 mm) of 8–16 serial sets of images during 120–180 s were obtained.

Image Analysis

$^{99m}TcO_4^-$ uptake in the tumor after acid stimulation was visually graded on static images as follows: grade 0 (no visible uptake); grade 1 (the uptake in the tumor was unclear); grade 2 (the uptake in the tumor was slightly visible); and grade 3 (the uptake in the tumor was clearly visible). Grading was done by 3 experienced nuclear medicine physicians (M.J., H.T., and Y.N. with 12, 11, and 25 years of experience, respectively); any disagreements were resolved by consensus. Grade 2 or 3 intensity was defined as positive.

MR images were reviewed and interpreted by 2 radiologists (M.J. and Y.F. with 12 and 18 years of experience, respectively). On T2-weighted images, the main findings for differential diagnosis were tumor hypointensity for Warthin tumor and tumor hyperintensity or isointensity for non-Warthin tumor, when compared with normal parotid tissue[10]. We evaluated whether the tumor had the hypointense area(s) characteristic of Warthin tumor. A region of interest (ROI) was set over the largest solid part of the tumor on each unenhanced and dynamic image to calculate the washout ratio (WR). The same size ROI was set over the same place of the tumor on each image. When no solid part was found in the tumor, ROIs were set over the cystic part of the tumor on the serial images. WR was calculated by a modified version of the method presented by Yabuuchi et al.[12] and Ikeda et al.[11] as follows:

$[(SI_{max} - SI_{120s})/(SI_{max} - SI_{pre})] \times 100$ (%), where SI_{max} was the signal intensity at maximal contrast enhancement, SI_{120s} was the signal intensity at 120 s after contrast material administration, and SI_{pre} was the precontrast unenhanced signal intensity.

Pathological Analysis

Each resected Warthin tumor was re-examined pathologically without knowledge of the results of $^{99m}TcO_4^-$ scintigraphy and MR imaging by a pathologist (T.Y., 8 years of experience for parotid tumors). Warthin tumors were classified into 4 subtypes: stroma-poor (70%–80% epithelial component), typical (40%–60% epithelial component), stroma-rich (20%–30% epithelial component) and metaplastic forms[8]. Tumor size was defined as the pathological maximum diameter of the tumor (n = 37).

Statistical Analysis

The Kruskal–Wallis test was used to evaluate the relationships between the degree of $^{99m}TcO_4^-$ uptake and the tumor size or histological subtype. The proportional test was used to compare the accuracy of $^{99m}TcO_4^-$ scintigraphy, T2-weighted MR imaging, and contrast-enhanced dynamic MR imaging for the diagnosis of Warthin tumor. A P value of <0.05 was considered statistically significant.

Results

Table 1 shows the results of $^{99m}TcO_4^-$ uptake grading in 83 parotid tumors after acid stimulation. The positive uptake (grade 2 or 3) was noted in 29 of 37 Warthin tumors (78%) and 1 of 46 non-Warthin tumors (2%). A marginal but not statistically significant positive relationship was found between the $^{99m}TcO_4^-$ uptake

Table 1. Visual Grading of $^{99m}TcO_4^-$ Uptake in 83 Parotid Lesions

Parotid Tumor		Grade of $^{99m}TcO_4^-$ Uptake			
	N	0	1	2	3
Warthin	37	5	3	7	22
Non-Warthin	46	42	3	1	0

Table 2. Correlation between Histological Subtype and Grade of $^{99m}TcO_4^-$ Uptake in Warthin Tumors

Histological Subtype		Grade of $^{99m}TcO_4^-$ Uptake			
	N	0	1	2	3
Stroma-poor	4	2	0	0	2
Typical	27	2	2	4	19
Stroma-rich	6	1	1	3	1
Metaplastic	0	0	0	0	0

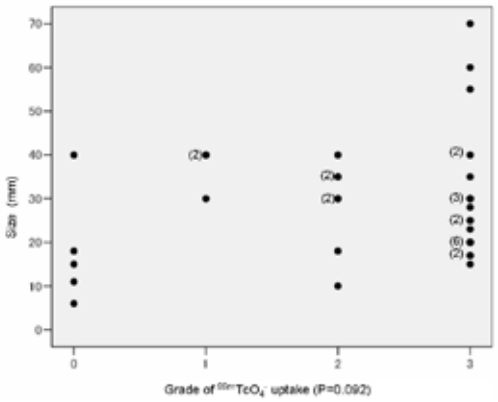

Fig. 1 The relationship between the grade of $^{99m}TcO_4^-$ uptake and the tumor size in Warthin tumors. The numbers in parentheses show the number of tumors.

grading and the histological subtype (P = 0.07) (Table 2). There was no case of the metaplastic form. No statistically significant relationship was found between the $^{99m}TcO_4^-$ uptake grading and the tumor size in Warthin tumors (P = 0.092) as shown in Figure 1.

Table 3 shows the contrast-enhanced dynamic MR imaging patterns in Warthin and non-Warthin tumors. The WR ≥30% in SI_{max} <65 s was the most frequent pattern in Warthin tumors [57% (12/20)]; we defined this pattern as the diagnostic criterion of Warthin tumor. Figure 2 shows the MR and scintigraphic images of a typical Warthin tumor. Figure 3 shows the MR and scintigraphic images of a typical non-Warthin tumor (pleomorphic adenoma).

Table 4 shows the diagnostic accuracy of $^{99m}TcO_4^-$ uptake, T2-weighted imaging, and washout ratios for the

Table 3. Contrast-enhanced Dynamic MRI Patterns in Warthin and Non-Warthin Tumors

		Contrast-enhanced dynamic MRI pattern				
Parotid Tumor	**N**	**SI_{max} <65 s**		**SI_{max} 65 – 119 s**	**SI_{max} ≥120 s**	**No Enhancement**
		WR ≥30%	**WR <30%**			
Warthin	20	12	2	3	1	2
Non-Warthin	30	1	3	2	22	2

SI_{max} indicates signal intensity at maximal contrast enhancement; WR, washout ratio.

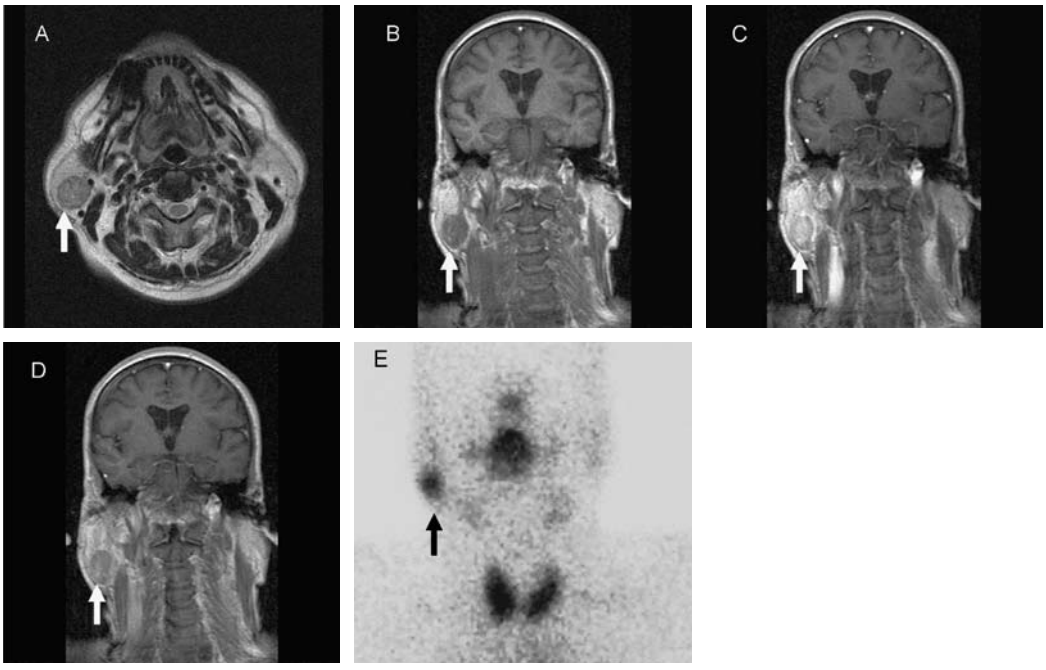

Fig. 2 MR and scintigraphic images of a typical Warthin tumor (in a 64-year-old male). The Warthin tumor shows a hypointense area lower in intensity than the intensity of the surrounding tissue of the right parotid gland in axial T2-weighted imaging (A arrow). Early enhancement and a high washout rate (70%) are seen on dynamic contrast-enhanced coronal MR imaging at 0 s (B arrow) and 43 s (C arrow). Rapid washout is observed 120 s after gadolinium chelate injection (D arrow). The Warthin tumor shows grade 3 uptake in $^{99m}TcO_4^-$ image (E arrow).

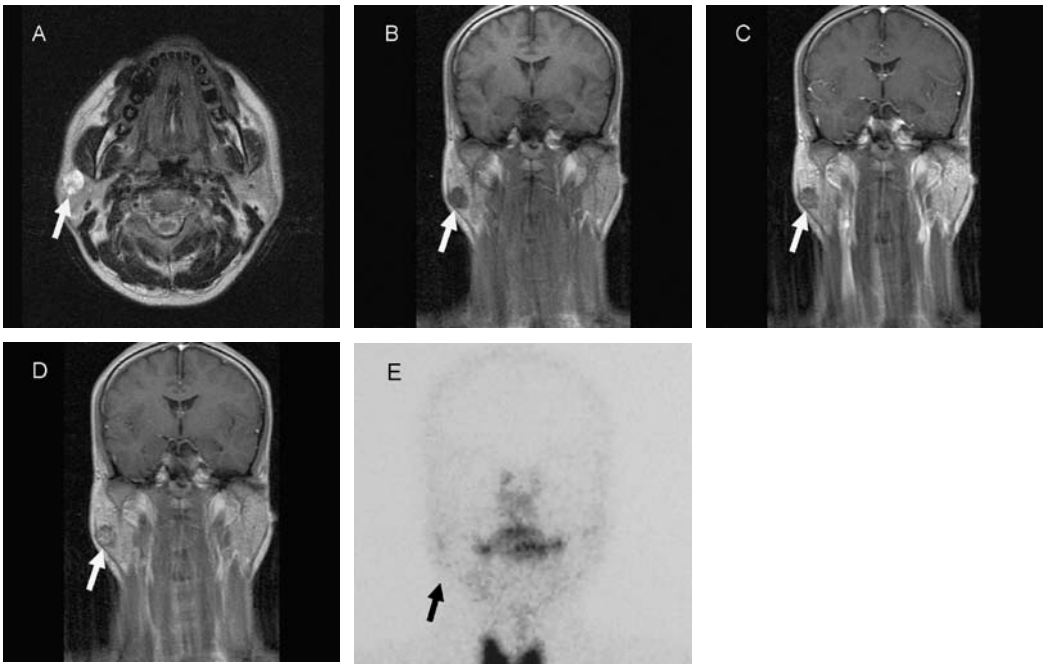

Fig. 3 MR and scintigraphic images of a typical non-Warthin tumor (pleomorphic adenoma) (in a 29-year-old male). The pleomorphic adenoma shows a hyperintense area, higher in intensity than the intensity of the surrounding tissue of the right parotid gland in axial T2-weighted imaging (**A** arrow). Gradual enhancement on dynamic contrast-enhanced coronal MR images is seen from 0 s (**B** arrow) to 42 s (**C** arrow). Peak enhancement is observed 120 s after gadolinium chelate injection (**D** arrow). The pleomorphic adenoma shows grade 0 uptake in $^{99m}TcO_4^-$ image (**E** arrow).

diagnosis of Warthin tumor. The diagnostic accuracy for Warthin tumor was higher in $^{99m}TcO_4^-$ scintigraphy (89%) than in T2-weighted imaging (81%) and contrast-enhanced dynamic MR imaging (82%), but statistically significant differences among them were absent ($P = 0.37$).

In $^{99m}TcO_4^-$ scintigraphy, a false-positive result (grade 2) was noted in the patient with metastasis of atypical meningioma (Figure 4A), which showed isointensity on T2-weighted imaging (Figure 4B); however, dynamic MR imaging data were not available for the same patient. Table 5 shows the summary of 8 $^{99m}TcO_4^-$ false-negative tumors. Of the 8 tumors, 6 had 1 or more nonviable pathological changes including: hemorrhage, hyaline or cystic degeneration, fibrosis, and infarction. Four tumors had the dynamic MR imaging data and none of the tumors showed the typical enhancement pattern (WR ≥30%) of Warthin tumor, but they showed other patterns such as no enhancement (n = 2), I_{max} ≥120 s (n = 1), SI_{max} <65 s and WR <30% (n = 1). Three of the 4 tumors showed hypointensity in T2-weighted imaging. In contrast-enhanced dynamic MR imaging, except for Warthin tumors, the enhancement pattern of WR ≥30% was found in 1 basal cell adenoma, which did not show $^{99m}TcO_4^-$ uptake. In the 8 Warthin tumors not showing the enhancement pattern of WR ≥30%, 5 were correctly diagnosed by $^{99m}TcO_4^-$ scintigraphy.

Table 4. Diagnostic Accuracy of $^{99m}TcO_4^-$ Scintigraphy and Magnetic Resonance Imaging (MRI) for Warthin Tumors

Examination	**Index of Diagnostic Accuracy (%)**		
	Sensitivity	**Specificity**	**Accuracy**
Scintigraphy*	78 (29/37)	98 (45/46)	89 (74/83)
T2-weighted MRI†	81 (17/21)	82 (27/33)	81 (44/54)
Dynamic MRI‡	60 (12/20)	97 (29/30)	82 (41/50)

Diagnostic criterion for Warthin tumor, *grade 2 or 3 $^{99m}TcO_4^-$ uptake,
†presence of hypointense area, ‡washout ratio ≥30%.

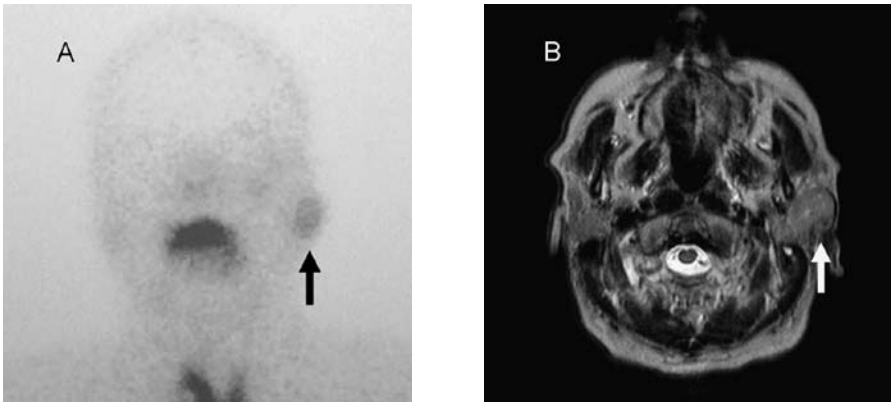

Fig. 4 A false-positive case of $^{99m}TcO_4^-$ scintigraphy for Warthin tumor (a metastatic tumor in the left parotid gland from an atypical meningioma in a 73-year-old male). The metastatic tumor shows grade 2 uptake in $^{99m}TcO_4^-$ scintigraphy (A arrow) and an isointensity area in T2-weighted imaging (B arrow).

Table 5. Summary of 8 $^{99m}TcO_4^-$ False-negative Warthin Tumor Lesions

Warthin Tumor Number	Patient Age/Sex	Pathological Finding			$^{99m}TcO_4^-$ Uptake Grade	Magnetic Resonance Imaging	
		Size (mm)	Subtype	Feature		T2 -weighted Hypointensity	Enhancement Pattern
1	68/M	6	Typical	Nothing particular	0	(−)	
2	54/M	11	Stroma-poor	Hemorrhage, hyaline degeneration	0	(−)	
3	70/M	18	Stroma-poor	Nothing particular	0	(−)	
4	60/F	18	Stroma-rich	Large cyst, fibrosis, hyaline degeneration	0	Absence	No enhancement
5	63/M	42	Typical	Infarction	0	Presence	No enhancement
6	50/M	40	Typical	Hyaline degeneration	1	(−)	
7	70/M	37	Typical	Large cyst, fibrosis	1	Presence	SI_{max}<65 s, WR <30%
8	57/M	32	Stroma-rich	Fibrosis, hyaline degeneration	1	Presence	SI_{max} ≥120 s

(−) indicates MR imaging was not performed,; SI_{max}, signal intensity at maximal contrast enhancement; WR, washout ratio.

Discussion

Warthin tumor is more common in men, occurs predominantly between the fifth and seventh decades of life, occurs predominantly in smokers, commonly presents as an asymptomatic painless swelling at the lower portion of the parotid gland, may be multicentric and/or develop bilaterally, is usually spherical to ovoid in shape, and is nearly always well circumscribed unless secondarily inflamed[1].

Warthin tumors retain $^{99m}TcO_4^-$ after acid stimulation

in contrast to pleomorphic adenomas and other benign and malignant salivary gland tumors. The usefulness of $^{99m}TcO_4^-$ scintigraphy with acid stimulation in detection of Warthin tumor has been reported and the sensitivity, specificity, and accuracy were reported to be 56%–100%, 91%–100%, and 87%–94%, respectively[3-6,10]. False-negative scans were reported in an entirely cystic tumor, a tumor adjacent to a large pleomorphic adenoma[6], and cystic or small tumors[10]. In our study, sensitivity was 78% and 8 false-negative cases were seen (Table 4). $^{99m}TcO_4^-$ uptake in Warthin tumor is thought to rely on the ability of epithelial cells in the tumor to extract large anions such as pertechnetate from the blood[2]. Because Warthin tumor does not communicate with the salivary ductal system, the accumulated $^{99m}TcO_4^-$ remains in the gland without being secreted[2, 7]. Therefore, we had initially speculated that $^{99m}TcO_4^-$ uptake might be positively related to tumor size and the amount of epithelial components of Warthin tumor. However, the degree of $^{99m}TcO_4^-$ uptake did not show statistically significant relationships with the tumor size and pathological subtype of Warthin tumors, although it showed marginally positive relationships with these 2 factors in our study. Miyake et al.[6] also found no statistically significant correlations between $^{99m}TcO_4^-$ uptake and the histological subtype; however, they found a statistically significant correlation between degree of $^{99m}TcO_4^-$ uptake and the tumor size of Warthin tumors and explained that large macroscopic cystic components were responsible for the lower $^{99m}TcO_4^-$ uptake. In our study, 2 Warthin tumors also had large cystic components showing lower $^{99m}TcO_4^-$ uptake (grade 0 or 1). One study explained that Warthin tumors with little or no accumulation of $^{99m}TcO_4^-$ may have less active epithelial cells[4]. Most of the false-negative tumors in our study had some level of pathological change such as hemorrhage, hyaline or cystic degeneration, fibrosis, and infarction. One explanation for the lower $^{99m}TcO_4^-$ uptake in Warthin tumors could be that these pathological changes.

Other parotid tumors that reportedly contain concentrated $^{99m}TcO_4^-$ include oncocytoma[6, 13], benign lymphoepithelial cyst[6], pleomorphic adenoma[6], acute sialoadenitis[14], epidermoid carcinoma[15], and acinic cell carcinoma[16]. In our study, the tumor in the patient with metastasis of atypical meningioma was false positive. Parotid metastasis of meningioma is very rare[17]. To our knowledge, the patient with parotid metastasis of atypical meningioma that took up $^{99m}TcO_4^-$ is the first such case reported. In contrast, it is a well- known fact that $^{99m}TcO_4^-$ concentrates in various types of brain tumors including benign and malignant meningiomas[18].

The MR imaging findings of parotid tumors have been described in several reports[11, 12, 19-21]. Ikeda et al.[11] summarized MR imaging findings of Warthin tumors. They explained that most Warthin tumors involve the inferior pole of the parotid gland and have a smooth margin on T1-weighted and T2-weighted MR imaging, sometimes showing characteristic hypointense areas on short T1 inversion recovery and T2-weighted MR imaging; in addition, they showed early enhancement and high WRs (>30%) in dynamic MR imaging and lower apparent diffusion coefficient values than those of the spinal cord in diffusion-weighted images. Working from the same institute as Ikeda et al.[11], Motoori et al.[10] compared the accuracy of $^{99m}TcO_4^-$ scintigraphy with citric acid or lemon juice stimulation and MR imaging by using receiver operating characteristic (ROC) curves and found that the mean area under the ROC curve was higher with MR imaging (0.97) than with $^{99m}TcO_4^-$ scintigraphy (0.88) for the diagnosis of Warthin tumor. In Motoori and colleagues' study[10], the diagnostic accuracy of Warthin tumors was evaluated by 2 observers who found that the specificity was high with both $^{99m}TcO_4^-$ scintigraphy (100%, 94%) and MR imaging (88%, 94%), but that the sensitivity was lower with $^{99m}TcO_4^-$ scintigraphy (56%, 63%) than with MR imaging (94%, 75%).

In our study, the diagnostic accuracy for Warthin tumor was higher with $^{99m}TcO_4^-$ scintigraphy with acid stimulation (89%) than with T2-weighted MR imaging (81%) and contrast-enhanced dynamic MR imaging (82%). However, we found no statistically significant differences between the three types of imaging and found the specificity to be higher than the sensitivity in $^{99m}TcO_4^-$ scintigraphy (98% vs. 78%), T2-weighted MR imaging (82% vs. 81%), and contrast-enhanced dynamic MR imaging (97% vs. 60%), suggesting that the criteria for scintigraphy and contrast-enhanced dynamic MR imaging for differentiating Warthin and non-Warthin tumors may have more value in terms of specificity than sensitivity. It is important to point out that we evaluated only the findings of T2-weighted MR imaging and contrast-enhanced dynamic MR imaging. It is possible that adding other findings such as those of Motoori and colleagues[10] obtained by T1-weighted and diffusion-weighted imaging may change the accuracy of MR imaging for the diagnosis of Warthin tumor.

In conclusion, $^{99m}TcO_4^-$ uptake in Warthin tumor does not appear to depend solely on tumor size or pathological subtype and may be affected by nonviable parenchymal changes including hemorrhage, hyaline or cystic degeneration, fibrosis, and infarction in the tumors. $^{99m}TcO_4^-$ scintigraphy may be equal to T2-weighted and contrast-enhanced MR imaging for differentiating Warthin and non -Warthin tumors.

Acknowledgements

We sincerely thank Dr. Chihaya Koriyama for her assistance with the statistical analysis. We also thank otolaryngologists and radiological technologists at Kagoshima university for their cooperation and Enago (www.enago.jp) for the English language review.

References

1) Ellis GL, Auclair PL: Warthin tumor. In: Silverberg SG, Sobin LH, eds. Tumors of salivary glands. AFIP Atlas of tumor pathology. Series 4; Fascicle 9. Washington, DC, American Registry of Pathology. 2008: 85-100.
2) Weinstein GS, Harvey RT, Zimmer W, Ter S, Alavi A: Technetium-99m pertechnetate salivary gland imaging: its role in the diagnosis of Warthin's tumor. J Nucl Med. 1994; 35: 179-183.
3) Sostre S, Medina L, de Arellano GR: The various scintigraphic patterns of Warthin's tumor. Clin Nucl Med, 1987; 620-626.
4) Yoshimura Y, Nohtomi M: Bilateral papillary cystadenoma lymphomatosum of the parotid gland without accumulation of technetium 99m pertechnetate: report of a case and review of the literature. J Oral Maxillofac Surg. 1991; 49: 401-404.
5) Murata Y, Yamada I, Umehara I, Okada N, Shibuya H: Diagnostic accuracy of technetium-99m-pertechnetate scintigraphy with lemon juice stimulation to evaluate Warthin's tumor. J Nucl Med. 1998; 39: 43-46.
6) Miyake H, Matsumoto A, Hori Y, Takeoka H, Kiyosue H, Hori Y, et al.: Warthin's tumor of parotid gland on Tc-99m pertechnetate scintigraphy with lemon juice stimulation: Tc-99m uptake, size, and pathologic correlation. Eur Radiol. 2001; 11: 2472-2478.
7) Siddiqui AR, Weisberger EC: Possible explanation of appearance of Warthin's tumor on I-123 and Tc-99m-pertechnetate scans. Clin Nucl Med. 1981; 6: 258-260.
8) Seifert G, Bull HG, Donath K. Histologic subclassification of the cystadenolymphoma of the parotid gland. Virchows Arch A Path Anat and Histol. 1980; 388: 13-38.
9) Sato T, Morita Y, Hamamoto S, Noikura T, Kawashima K, Matsune S, et al.: Interpretation of scintigraphy of papillary cystadenoma lymphomatosum (Warthin's tumor) on the basis of histopathologic findings. Oral Surg Oral Med Oral Pathol Oral Radiol Endod. 1996; 82: 101-107.
10) Motoori K, Ueda T, Uchida Y, Chazono H, Suzuki H, Ito H: Identification of Warthin tumor Magnetic resonance imaging versus salivary scintigraphy with technetium-99m pertechnetate. J Comput Assist Tomogr. 2005; 29: 506-512.
11) Ikeda M, Motoori K, Hanazawa T, Nagai Y, Yamamoto S, Ueda T, et al.: Warthin tumor of the parotid gland: diagnostic value of MR imaging with histopathologic correlation. AJNR Am J Neuroradiol. 2004; 25: 1256-1262.
12) Yabuuchi H, Fukuya T, Tajima T, Hachitanda Y, Tomita K, Koga M: Salivary gland tumors: diagnostic value of gadolinium-enhanced dynamic MR imaging with histopathologic correlation. Radiology. 2003; 226: 345-354.
13) Ausband JR, Kittrell BJ, Cowen RJ: Radioisotope scanning for parotid oncocytoma. Arch Otolaryngol Head and Neck Surg. 1971; 93: 628-629.
14) Liu R, Yeh S, Yen T, Hsu D: Salivary scintigraphy with vitamin C stimulation: an aid in differentiating unilateral parotitis from Warthin's tumor. Eur J Nucl Med. 1990; 16: 689-691.
15) McGuirt WF, McCabe BF: Limitation of parotid scans. Ann Otol Rhinol Laryngol. 1977; 86: 247-250.
16) Dosoretz C, Lieberman LM. Increased uptake of Tc-99m pertechetate in a salivary gland cancer. Clin Nucl Med. 1987; 12: 944-945.
17) Celli P, Palma L, Domenicucci M, Scarpinati M: Histologically benign recurrent meningioma metastasizing to the parotid gland: case report and review of the literature. Neurosurgery. 1992; 31: 1113-1116.
18) Schwartz ML, Tator CH. Shortcomings of ^{99m}Tc-pertechnetate as a tracer for brain tumor detection as shown by well counting of human tumors and a mouse ependymoblastoma. J Nucl Med. 1972; 13:

321-327.

19) Tsushima Y, Matsumoto M, Endo K: Parotid and parapharyngeal tumors: tissue characterization with dynamic magnetic resonance imaging. Br J Radiol. 1994; 67: 342-345

20) Swartz JD, Rothman MI, Marlowe FI, Berger AS: MR imaging of parotid mass lesions: attempts at histopathologic differentiation. J Comput Assist Tomogr. 1989; 13: 789-796.

21) Som PM, Biller HF: High-grade malignancies of the parotid gland: identification with MR imaging. Radiology. 1989; 173: 823-826.

ワルチン腫瘍の診断における酸負荷唾液腺シンチグラフィの集積とMRI所見や病理組織所見との比較

神宮司メグミ[1)]，田邉　博昭[1)]，中條　政敬[1)]，中別府良昭[1)]，福倉　良彦[1)]，松根　彰志[2)]，義岡　孝子[3)]

[1)] 鹿児島大学大学院医歯学総合研究科　先進治療科学専攻　腫瘍学講座　放射線診断治療学，
[2)] 同感覚器病学講座　耳鼻咽喉科・頭頸部外科学，
[3)] 同腫瘍学講座　分子細胞病理学

目的：^{99m}Tc pertechnetateによる酸負荷唾液腺シンチグラフィ検査での集積程度がワルチン腫瘍の大きさや組織学的亜型と関連があるかを調べ，更に耳下腺のワルチン腫瘍と非ワルチン腫瘍の鑑別について，酸負荷唾液腺シンチグラフィとMRI検査の診断能を比較した。
方法：酸負荷唾液腺シンチグラフィと手術が行われた79名の患者（ワルチン腫瘍37個，非ワルチン腫瘍46個）について後顧的にシンチグラフィの集積程度を視覚的に評価した。これらのうち53名が術前にMRI検査を受けており（ワルチン腫瘍21個，非ワルチン腫瘍33個），ダイナミック造影が50名（ワルチン腫瘍20個，非ワルチン腫瘍30個）になされていた。ワルチン腫瘍の大きさや組織学的亜型（上皮成分の割合70－80%，40－60%，20－30%）と酸負荷唾液腺シンチグラフィの集積程度との関連を調べた。次にワルチン腫瘍か非ワルチン腫瘍かの診断能について，MRIのT2強調像とダイナミック造影像の所見を評価した。また，ワルチン腫瘍の診断における酸負荷唾液腺シンチグラフィとMRIのT2強調像とダイナミック造影像について，正診率を統計学的に比較した。
結果：ワルチン腫瘍における腫瘍の大きさや組織学的亜型と酸負荷唾液腺シンチグラフィでの集積程度との間にはいずれにおいても統計学的な有意差は得られなかった（P=0.092，P=0.070）。８例の偽陰性例の中には６例が出血や硝子化，嚢胞変性，線維化，梗塞といった何らかの変性を伴っていた。異型性髄膜腫の転移の１例が偽陽性であった。それぞれの正診率については酸負荷唾液腺シンチグラフィが89%（感度78%，特異度98%），MRIのT2強調像が81%（感度81%，特異度82%），MRIのダイナミック像が82%（感度60%，特異度97%）であり，これらの検査間での診断能に統計学的な有意差は得られなかった（P=0.37）。
結論：ワルチン腫瘍における酸負荷唾液腺シンチグラフィでの集積は腫瘍の大きさや組織学的亜型のみが関与するわけではなく，出血や腫瘍の非活動性的な実質の変性によっても影響される可能性が考えられた。酸負荷唾液腺シンチグラフィにおけるワルチン腫瘍と非ワルチン腫瘍の診断能はMRIでのT2強調像やダイナミック造影検査とほぼ同等であった。